Supporting Information

High-efficiency Methanol Oxidation Electrocatalyst Realized by Ultrathin PtRuM-O (M = Ni, Fe, Co) Nanosheets

Yue Pan,[#] Hongdong Li,[#] Zuochao Wang, Yi Han, Zhanchao Wu, Xinyi Zhang, Jianping Lai,* Lei Wang* and Shouhua Feng

Key Laboratory of Eco-chemical Engineering, Ministry of Education, Taishan scholar advantage and characteristic discipline team of Eco-chemical process and technology, Laboratory of Inorganic Synthesis and Applied Chemistry, College of Chemistry and Molecular Engineering, Qingdao University of Science and Technology, Qingdao 266042, P. R. China

E-mail: jplai@qust.edu.cn; inorchemwl@126.com

[#] Equal Contribution

19 August 2021
Note added after first publication:
This supplementary information file replaces that originally published on 13 June 2020. The specific activity value for the Pt_7RuNi_2-O NS catalyst in Table S1 was incorrect in the original version. The correct value is 4.65 mA cm^{-2} as shown in this corrected version.

Experimental Section

Chemicals

$Pt(acac)_2$ (97%), $Ni(acac)_2$ (95%) were bought from Sigma-Aldrich. $Fe(acac)_3$ (99+%), $Ru(acac)_3$ (Ru 24% min) were purchased from Alfa Aesar. $Co(acac)_3$ (>98%) from TCI. Cetyltrimethylammonium bromide was provided by Angie Chemical Company. Oleyl amine, molybdenum hexacarbonyl were bought from Sigma-Aldrich. All chemicals were not further processed when used. Ultrapure water (Millipore Milli-Q grade) with a resistivity of 18.2 MΩ was used in all the experiments.

Synthesis of ultrathin Pt_7Ru_3 Nnaosheets (NSs)

4.0 mL of oleylamine, $Pt(acac)_2$ (20 mg, 0.051 mmol), $Ru(acac)_3$ (8.7 mg, 0.022 mmol), and cetyltrimethylammonium bromide (CTAB) (50 mg, 0.137 mmol) were added to a 15.0 mL pressure bottle, preheated for 5 minutes in an oil bath at 200 ℃. $Mo(CO)_6$ (20 mg, 0.076 mmol) was then quickly added to the reaction. The reaction was quenched after 2 hours and washed three times with a mixture of ethanol and cyclohexane to obtain the product.

Synthesis of ultrathin Pt_7RuM_2(M=Fe, Co, Ni) NSs

Adding 4.0 mL of oleylamine solution, $Pt(acac)_2$ (20 mg, 0.051 mmol), $Ru(acac)_3$ (2.0 mg, 0.005 mmol), $Ni(acac)_2$ (4.4 mg), 0.017 mmol) and cetyltrimethylammonium bromide (CTAB) (50 mg, 0.137 mmol) to a 15.0 mL pressure bottle, preheated in a 200 ℃ oil bath for 5 min. $Mo(CO)_6$ (20 mg, 0.076 mmol) was then quickly added to the reaction. The reaction was terminated after 2 hours, and the mixture was washed three times with a mixture of ethanol and cyclohexane to obtain a product. Different metal materials can be prepared by maintaining the same amount of Pt and Ru, and then adding the same molar ratio of different metals (Co, Fe). Different ratios of materials were prepared by adjusting the ratios of Ru and Ni (Pt_7Ru_2Ni, Pt_7RuNi_2, $Pt_7Ru_{0.5}Ni_{2.5}$) in molar ratio.

Characterization

X-ray diffraction (XRD) analysis in the 2θ ranges from 4 °to 80 °was used to examine the compositions and crystal structure of the as-synthesized samples. Transmission electron microscopy (TEM), high-resolution TEM (HRTEM) measurements TEM-mapping and TEM-EDX were performed on FEI Tecnai-G2 F30 at an accelerating voltage of 300 KV. X-ray photoelectron spectrum (XPS) was conducted using a VG ESCALABMK II spectrometer with Al Ka (1486.6 eV) photon source. The proportion of elements in the catalysts were determined by the inductively coupled plasma atomic emission spectrometer (Varian 710-ES).

Electrochemical measurements

Before testing, the material should be loaded with Ketchen carbon black (about 20 wt%), mixed and sonicated in an ultrasonic cleaner for more than 1 hour to fully load the sample with Ketjen carbon black.

After ultrasonication, it is placed in a centrifuge for centrifugation, and then dried in an oven. After the composite sample is dried, it is taken in a porcelain boat and placed in a muffle furnace and calcined at a high temperature of 220 ^{o}C for more than 1 hour to remove residual surfactant on the surface. After dropping to room temperature, weigh 1 mg as-synthesized samples were added into 0.5 mL isopropanol and 0.5 mL H_2O with 10 μL Nafion and supersonic dispersion to obtain sample solution of 1 mg mL^{-1}.

All electrochemical tests were carried out in a conventional electrolytic cell, and the data was collected and processed using the CHI 760E electrochemical workstation of Shanghai Chenhua Company. The experiment was carried out using a classical three-electrode system with an Ag/AgCl electrode as the reference electrode, a graphite rod as the counter electrode, and a glass carbon electrode (GCE) as the working electrode. Before depositing, the electrodes were polished using 0.5 μm Al_2O_3 and 50 nm Al_2O_3. After grinding, ultrasound was performed in ultrapure water. 10 μL of the dispersed sample was dropped on the electrode and naturally dried at room temperature to form a uniform sample film.

After that, a series of electrochemical tests were performed. The samples were activated by cyclic voltammetry (CV) test in 0.5 M sulfuric acid with a scan rate of 50 mV s^{-1}. And after the activation, the ECSA test was performed in 0.5 M sulfuric acid at 20 mV s^{-1}. The methanol oxidation reaction (MOR) test was carried out in a mixed solution of 0.5 M sulfuric acid and 0.5 M methanol by CV at a sweep rate of 20 mV s^{-1}. The stability of samples was performed through 1000 CV cycles and chronoamperometry (i-t curve) test. I-t test was measured in a mixed solution of 0.5 M sulfuric acid and 0.5 M methanol with a voltage setting of 0.85 V *vs.* RHE and a test time of 8000 s. The CO stripping voltammetry test was carried out in 0.5 M sulfuric acid, and N_2 gas (or Ar gas) was passed for more than 20 min before the experiment. The CO gas was then subjected to i-t test at -0.1 V *vs.* RHE for 900 s. After the end, N_2 gas (or Ar gas) was passed for more than 20 min, and the test was carried out at a sweep speed of 20 mV s^{-1} in 0.5 M sulfuric acid. All the potentials here were referenced to a reversible hydrogen electrode (RHE): E(RHE) = E(Ag/AgCl) + 0.197 V.

Supplementary Figures and Tables

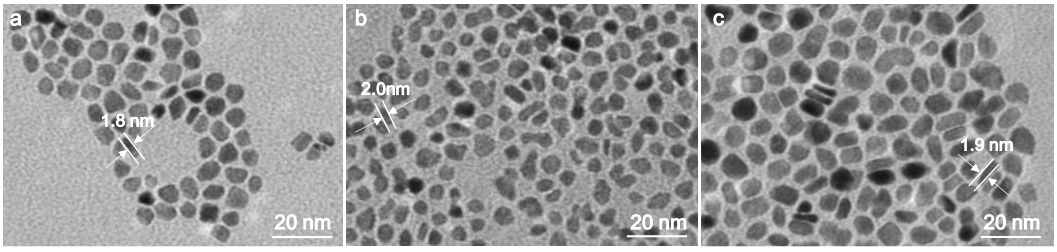

Fig. S1. TEM images (a) Pt_7RuNi_2-O NSs, (b) Pt_7RuFe_2-O NSs, (c) Pt_7RuCo_2-O NSs.

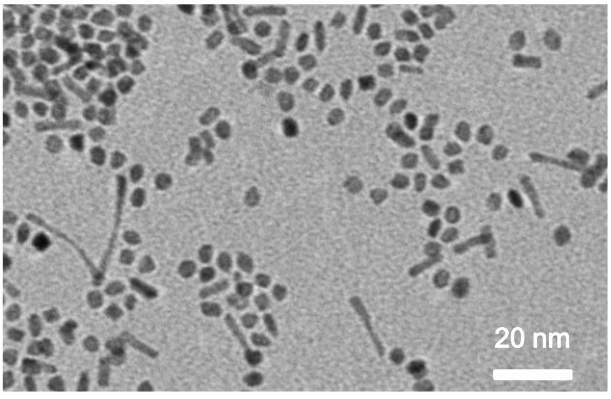

Fig. S2. TEM image of $Pt_7Ru_{0.5}Ni_{2.5}$-O material. It can be seen that when the proportion of Ni increases, the morphology will change, and a small number of nanowires were synthesized.

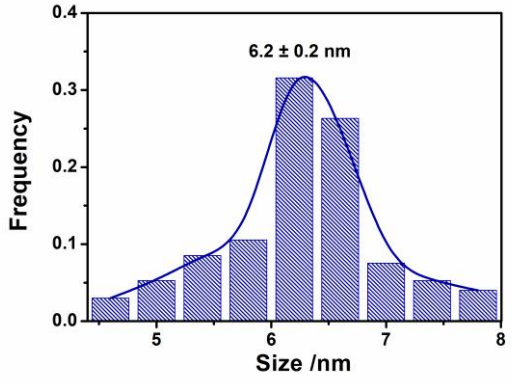

Fig. S3. The diameter distribution histogram of Pt_7RuNi_2-O NSs material.

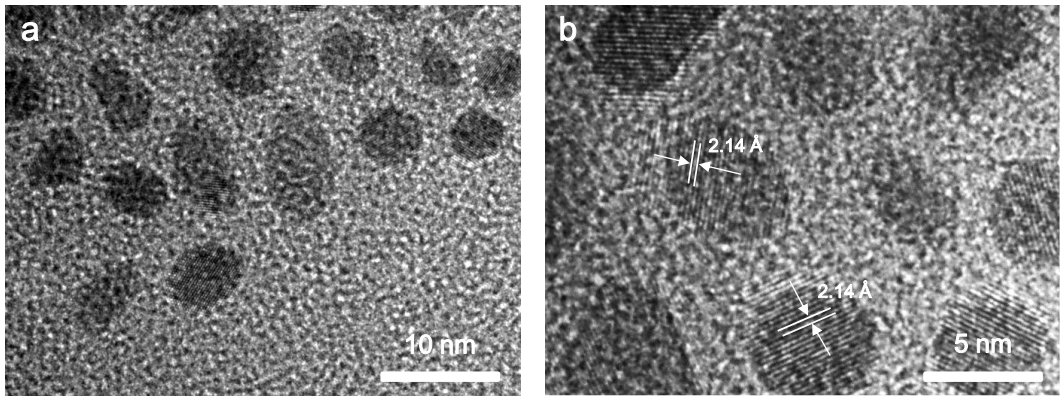

Fig. S4. (a) TEM and (b) HRTEM images of Pt_7RuFe_2-O NSs.

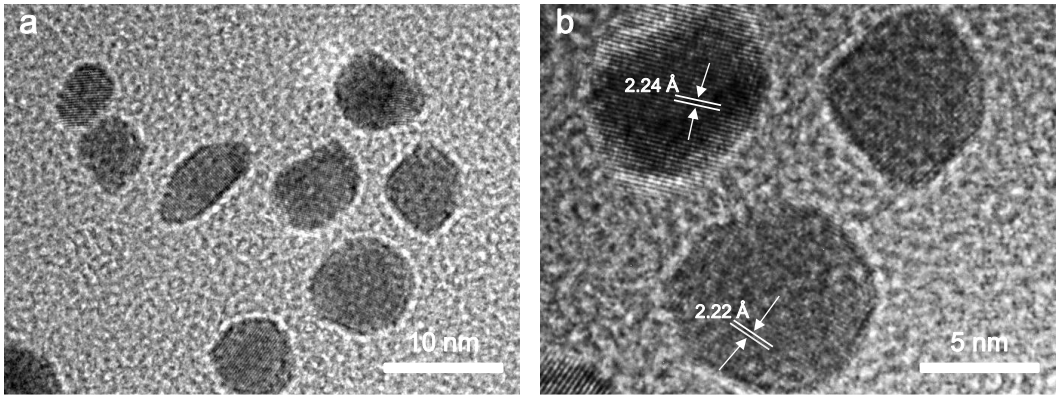

Fig. S5. (a) TEM and (b) HRTEM images of Pt_7RuCo_2-O NSs.

It can be seen from **Fig. S4b** and **S5b** that the lattice fringes of Pt_7RuFe_2-O NSs and Pt_7RuCo_2-O NSs are also about 2.14 Å and 2.22 Å, also corresponding to the (111) lattice plane of fcc alloy.

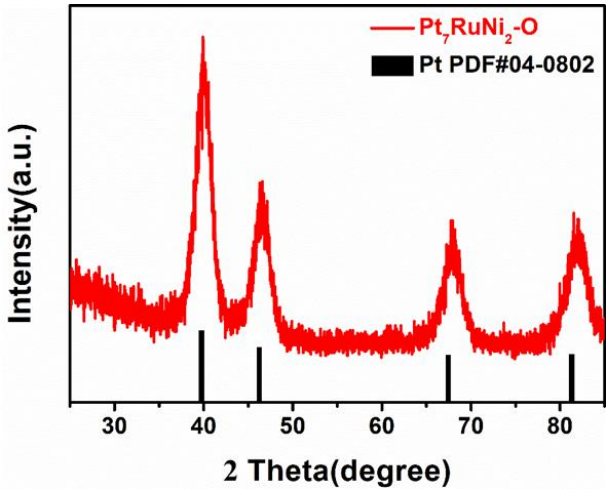

Fig. S6. XRD pattern of Pt_7RuNi_2-O material.

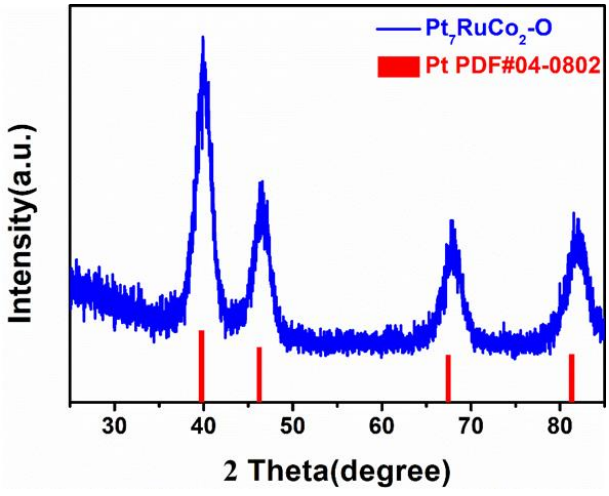

Fig. S7. XRD pattern of Pt_7RuCo_2-O material.

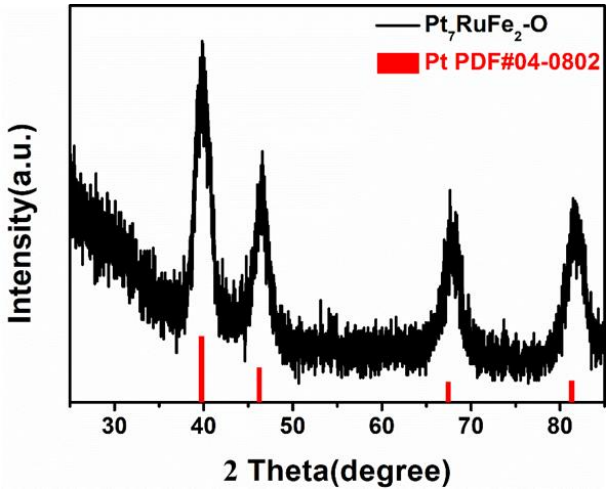

Fig. S8. XRD pattern of Pt_7RuFe_2-O material.

To further know about crystal characters of prepared nanomaterials, the XRD spectrums of Pt_7RuNi_2-O NSs **(Fig. S6)**, Pt_7RuCo_2-O NSs **(Fig. S7)**, and Pt_7RuFe_2-O NSs (**Fig. S8**) materials were analyzed, where the peaks located at 39.7 °, 46.2 °, 67.5 °, and 81.2 °are the characteristic peaks of the (111), (200), (220) and (311) planes of fcc crystal, respectively. And the patterns are devoid of the elemental Ru, Ni, Fe or Co peaks, thereby suggesting that the uniform alloys can be formed by the reduction of the precursor.

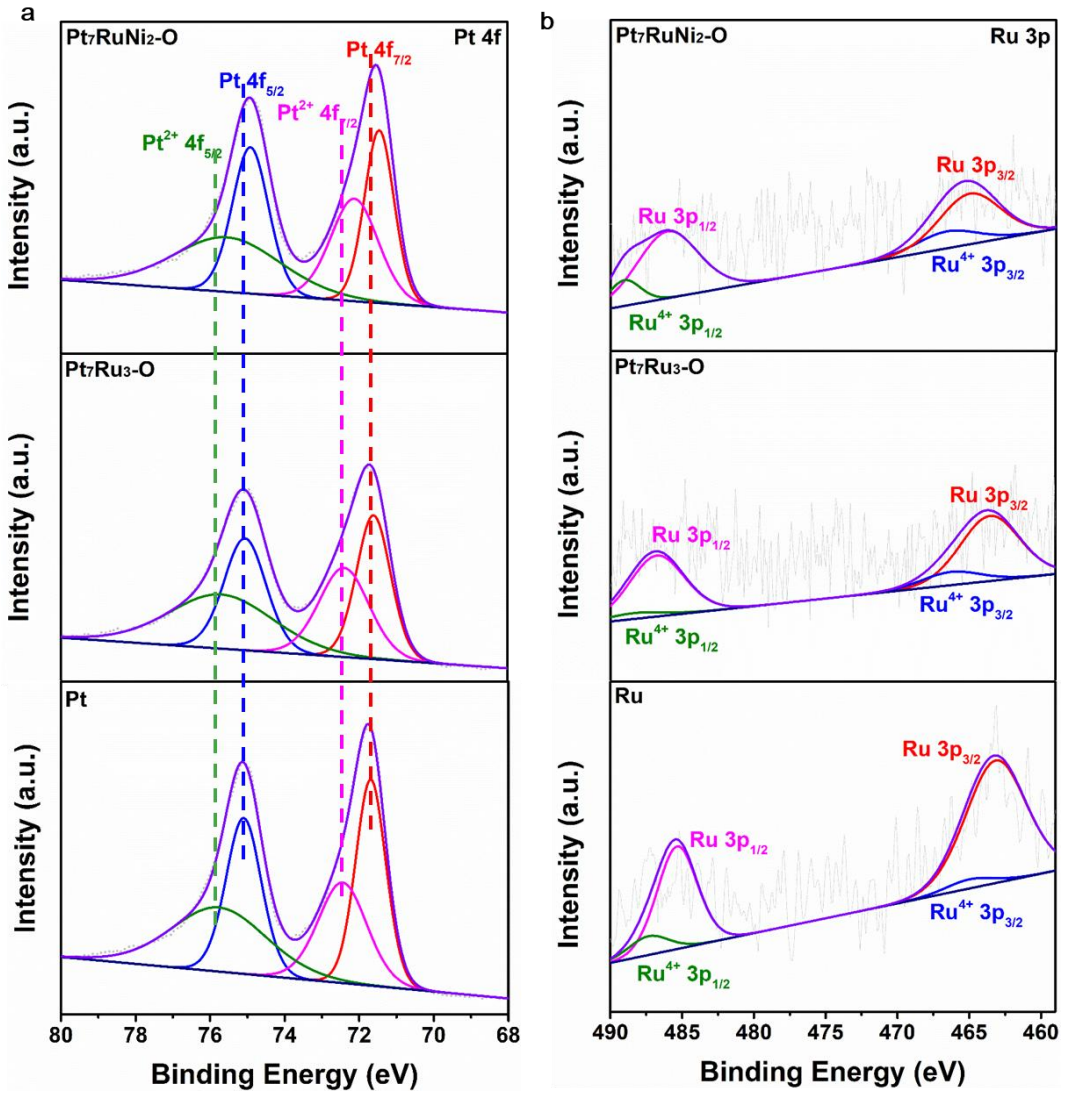

Fig. S9. High-resolution XPS spectral contrast of (a) Pt 4f and (b) Ru 3p of Pt_7RuNi_2-O (up), Pt_7Ru_3-O (middle) NSs and pure Pt and pure Ru (down).

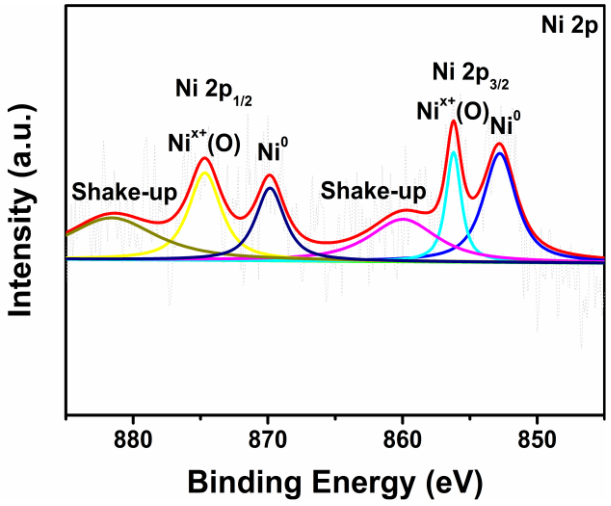

Fig. S10. High-resolution Ni 2p XPS spectral of Pt_7RuNi_2-O NSs.

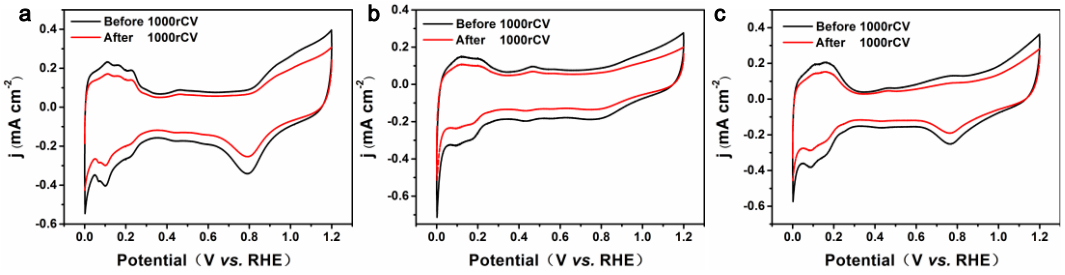

Fig. S11. CV profiles of (a) Pt_7RuNi_2-O (b) Pt_7Ru_2Ni-O (c) $Pt_7Ru_{0.5}Ni_{2.5}$-O recorded in N_2-saturated 0.5 M H_2SO_4 solution at a sweep rate of 20 mV s^{-1}.

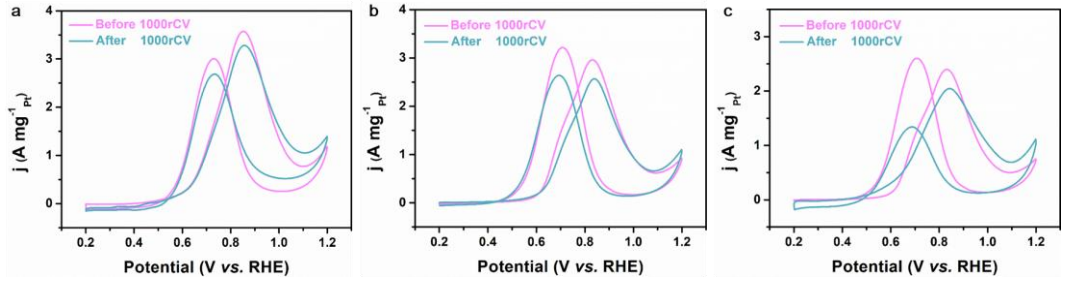

Fig. S12. CV curves of (a) Pt_7RuNi_2-O catalyst, (b) Pt_7Ru_2Ni-O catalyst and (c) $Pt_7Ru_{0.5}Ni_{2.5}$-O catalyst before and after 1000 cycles.

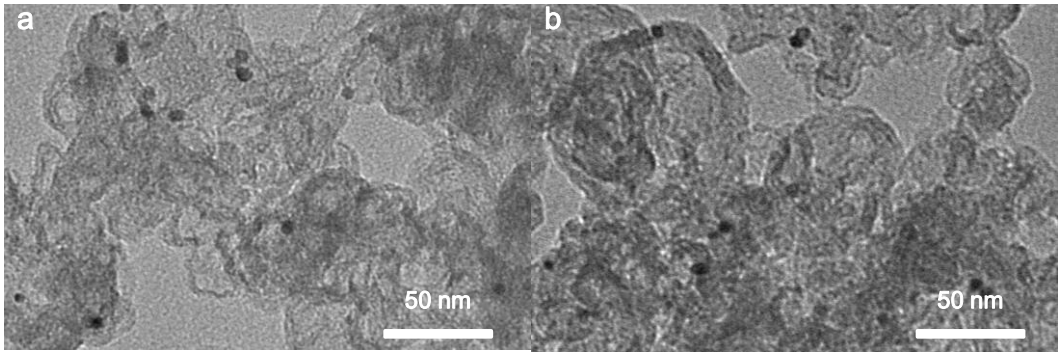

Fig. S13. TEM images of electrochemical test before reaction (a) and after reaction (b) of Pt_7RuNi_2-O/C catalyst.

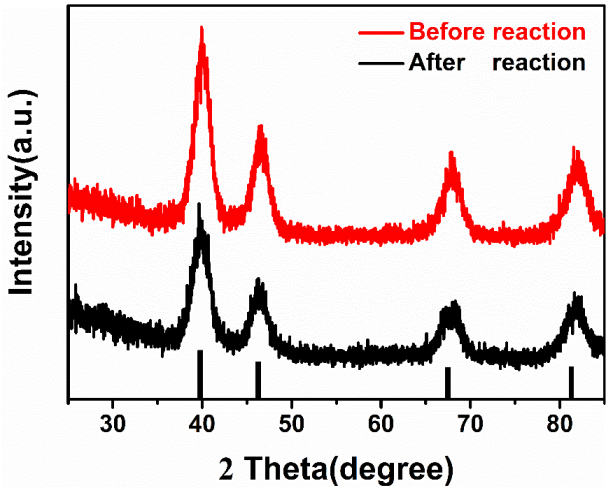

Fig. S14. XRD patterns of Pt_7RuNi_2-O material before and after MOR stability test.

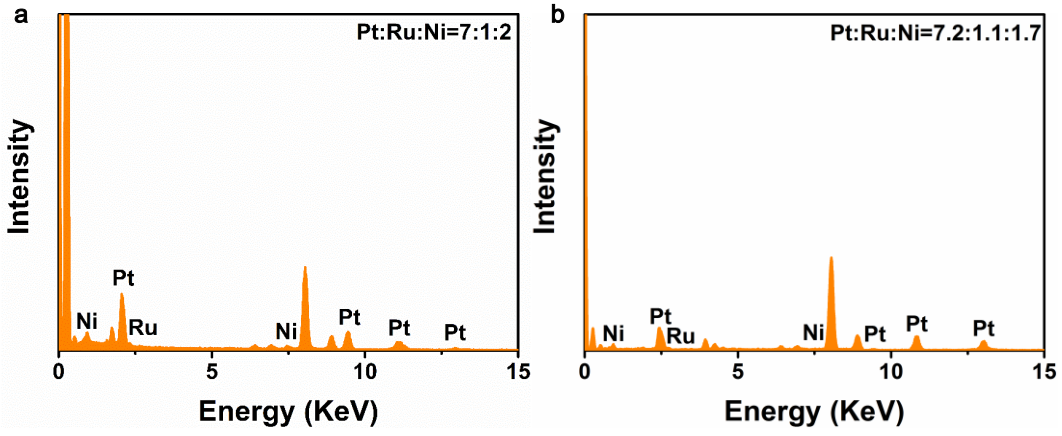

Fig. S15. EDX patterns of Pt_7RuNi_2-O material before and after MOR stability test.

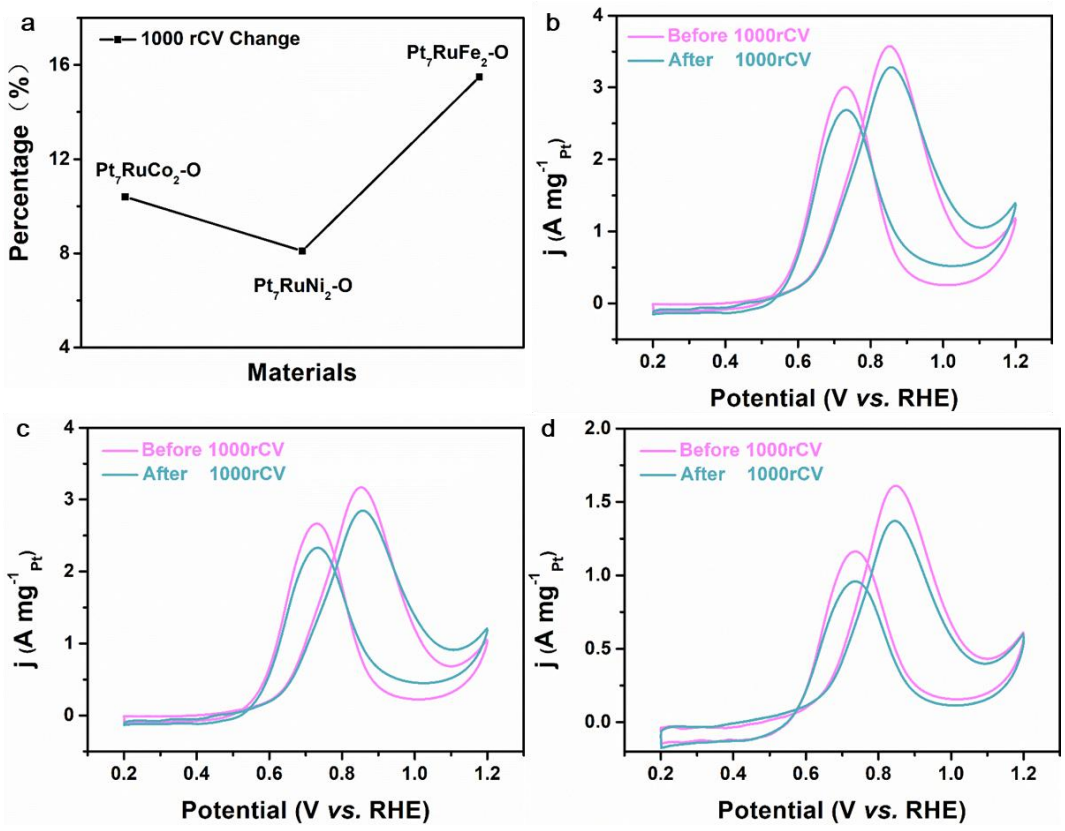

Fig. S16. Comparison of MOR performance before and after 1000 CV. (a) Percentage contrast line chart of mass activity reduction of three materials before and after 1000 CV cycles. CV curves of (b) Pt_7RuNi_2-O catalyst, (c) Pt_7RuCo_2-O catalyst and (d) Pt_7RuFe_2-O catalyst before and after 1000 CV cycles.

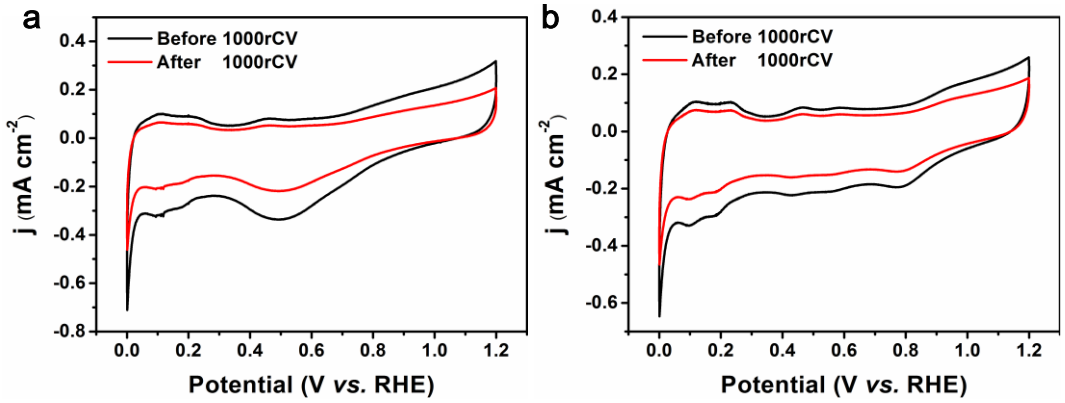

Fig. S17. CV profiles of (a) Pt_7RuFe_2-O (b) Pt_7RuCo_2-O recorded in N_2-saturated 0.5 M H_2SO_4 solution at a sweep rate of 20 mV s^{-1}.

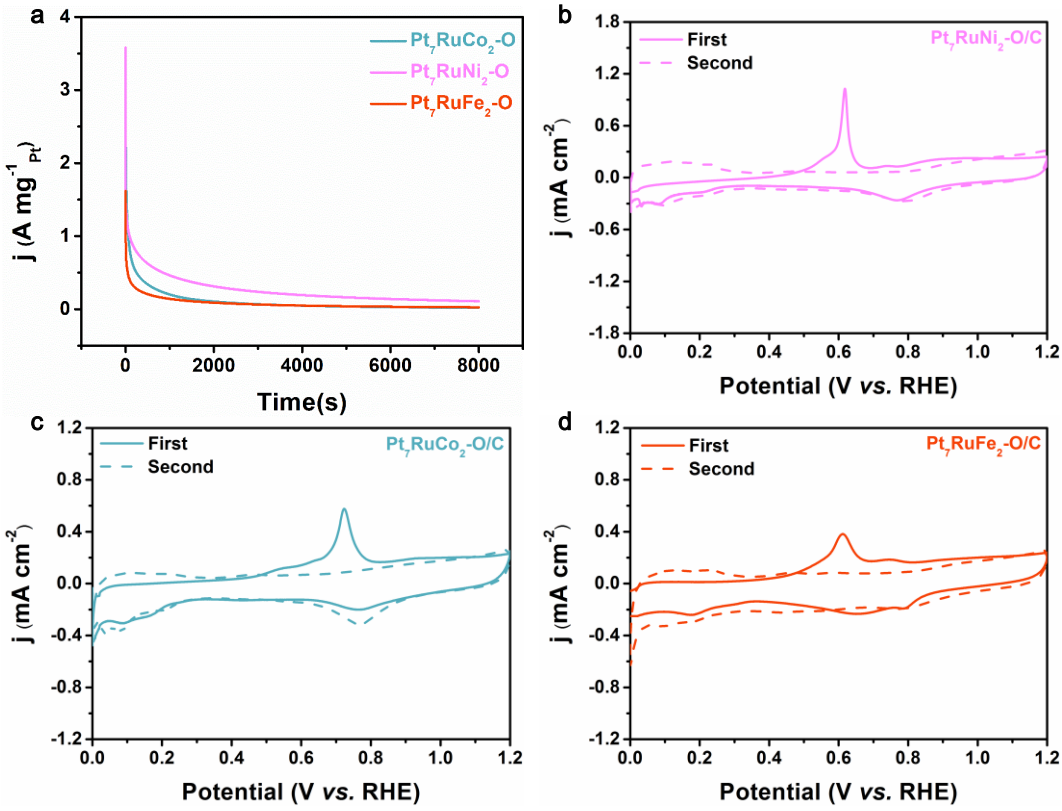

Fig. S18. (a) i-t test curves of Pt_7RuNi_2-O, Pt_7RuCo_2-O, and Pt_7RuFe_2-O catalysts; CO stripping test curves of (b) Pt_7RuNi_2-O, (c) Pt_7RuCo_2-O, and (d) Pt_7RuFe_2-O catalysts.

We also compared the stability and anti-poisoning properties of PtRuM-O (Fe, Co, and Ni) electrocatalysts through the 1000 CV cycles test (**Fig. S16** and **Fig. S17**), i-t test (**Fig. S18a**), and CO stripping test (**Fig. S18b-d**). The mass activity of Pt_7RuCo_2-O NS, and Pt_7RuFe_2-O NS catalysts was reduced by 10.4%, and 15.5% after 1000 CVs, respectively.

Table S1. Some recently reported representative Pt-based electrocatalysts for MOR under acidic conditions. All the specific/mass activities represent the forward peak current densities of different catalysts except the values noted at a certain potential.

Catalysts	Electrolyte	Mass Activity ($A\ mg^{-1}$)	Specific Activity ($mA\ cm^{-2}$)	Ref.
Pt_7RuNi_2-O NSs	**0.5 M H_2SO_4 + 0.5 M CH_3OH**	**3.57**	**4.65**	**This Work**
CoPtAu nanoparticle	0.1 M $HClO_4$ + 2 M CH_3OH	1.49	-	[1]Angew. Chem. Int. Ed., 2019, 131, 11651.
RuO_x-decorated RuPtCu hetero nanocages	0.1 M $HClO_4$ + 1.0 M CH_3OH	1.73	4.52	[2]Nanoscale, 2018, 10, 21178.
Pt/Mo_2C NTs	0.5 M H_2SO_4 + 0.5 M CH_3OH	-	1.52	[3]NPG Asia Mater., 2015, 7, e153.
High crystalline opened PtCu Nanotubes	0.5 M H_2SO_4 + 1.0 M CH_3OH	2.252	6.09	[4]Energy Environ. Sci., 2017, 10, 1751.
Pt NW/N-doped low-defect graphene	1.0 M $HClO_4$ + 2.0 M CH_3OH	1.283	-	[5]Small, 2017, 13, 1603013.
PtRu/TiWC NPs	0.1 M $HClO_4$ + 1.0 M CH_3OH	-	~1.8	[6]Science, 2016, 352, 974.
PtPb/Pt nanoplate	0.1 M $HClO_4$ + 0.1 M CH_3OH	1.500	~2.6	[7]Science, 2016, 354, 1410.
Pt-Ni_2P/C	0.5 M $HClO_4$ + 1.0 M CH_3OH	1.432	4.05	[8]Energy Environ. Sci., 2014, 7, 1628.
Ru decorated Pt icosahedra	0.5 M H_2SO_4 + 0.5 M CH_3OH	0.074	0.76	[9]Nanoscale, 2016, 8, 12812.
PtCo NWs	0.1 M $HClO_4$ + 0.2 M CH_3OH	1.020	1.96	[10]Nat. Commun., 2016, 7, 11850.
PtRu/Cu NWs	0.1 M $HClO_4$ + 1.0 M CH_3OH	-	1.60	[11]ACS Catal., 2015, 5, 1468.
$Pt_{62}Ru_{18}Ni_{20}$-O/C NWs	0.5 M H_2SO_4 + 0.5 M CH_3OH	2.72	4.36	[12]J. Mater. Chem. A, 2020, 8, 2323-2330.

References

[1] J. Li, S. Z. Jilani, H. Lin, X. Liu, K. Wei, Y. Jia, P. Zhang, M. Chi, Y. Tong, X. Zheng, S. Sun, *Angew. Chem. Int. Ed.*, 2019, **131**, 11651-1165.

[2] J. Park, H. Kim, A. Oh, T. Kwon, H, Baik, S. Choi, K. Lee, *Nanoscale*, 2018, **10**, 21178-21185.

[3] K. Zhang, W. Yang, C. Ma, Y. Wang, C. Sun, Y. Chen, P. Duchesne, J. Zhou, J. Wang, Y. Hu, M. N. Banis, P. Zhang, F. Li, J. Li and L. Chen, *NPG Asia Mater.*, 2015 **7**, e153.

[4] H. Li, Q. Fu, L. Xu, S. Ma, Y. Zheng, X. Liu and S. Yu, *Energy Environ. Sci.*, 2017, **10**, 1751-1756.

[5] H. Huang, L. Ma, C. Tiwary, Q. Jiang, K. Yin, W. Zhou and P. Ajayan, *Small*, 2017, **13**, 1603013.

[6] S. Hunt, M. Milina, A. Alba-Rubio, C. Hendon, J. Dumesic and Y. Leshkov, *Science*, 2016, **352**, 974-978.

[7] L. Bu, N. Zhang, S. Guo, X. Zhang, J. Li, J. Yao, T. Wu, G. Lu, J. Ma, D. Su and X. Huang, *Science*, 2016, **354**, 1410-1414.

[8] J. Chang, L. Feng, C. Liu, W. Xing and X. Hu, *Energy Environ. Sci.*, 2014, **7**, 1628-1632.

[9] Z. Lin, W. Chen, Y. Jiang, T. Bian, H. Zhang, J. Wu, Y. Wang and D. Yang, *Nanoscale*, 2016, **8**, 12812-12818.

[10] L. Bu, S. Guo, X. Zhang, X. Shen, D. Su, G. Lu, X. Zhu, J. Yao, J. Guo and X. Huang, *Nat. Commun.*, 2016, **7**, 11850.

[11] J. Zheng, D. Cullen, R. Forest, J. Wittkopf, Z. Zhuang, W. Sheng, J. Chen and Y. Yan, *ACS Catal.*, 2015, **5**, 1468-1474.

[12] H. Li, Y. Pan, D. Zhang, Y. Han, Z. Wang, Y. Qin, S. Lin, X. Wu, H. Zhao, J. Lai, B. Huang and L. Wang, J. Mater. Chem. A, 2020, 8, 2323-2330.